CONTINUOUS COMMISIONING BASED ON EXTENDED FAULT DETECTION AND DIAGNOSIS

Gerhard Zimmermann[1], Yan Lu[2] and George Lo[2]

[1]Informatik, University of Kaiserslautern, Germany

[2] Siemens Corporation, Corporate Research, Princeton, USA

ABSTRACT

Buildings seldom perform as intended, resulting in energy use much higher than predicted from design. State-of-the-art HVAC fault detection and diagnosis (FDD) systems report component failures that may corrupt energy efficiency, however FDD does not detect component performance degradation and energy waste from poor designed control sequences. This paper introduces energy related extensions to our previous HFM-FDD system, with which energy consumption/production is modeled and simulated in HFM (Heat Flow Model) nodes. The inconsistency between simulated energy data and measured data indicates component performance degradation. In addition, alternative control strategies (control algorithms, set-points, etc.) are modeled in the HFM simulation engine to test energy optimization opportunities. All energy calculations can be averaged with short term real data histories. Full year energy evaluations can be produced using standard or local weather files. These extensions that include air and water flow nodes support continuous commissioning® (CCx) with operation optimization. The HFM-FDD with energy and control modeling extension is designed as generic as possible, and requires minimal engineering efforts because of model based software generation techniques. Results using structure and data from a complex HVAC system of a real building are included.

MOTIVATION

Building commissioning includes, according to ASHRAE, the initial commissioning after construction, retro-commissioning of existing buildings, and the continuous commissioning® during the lifecycle of the building. In the case of complex HVAC systems, the initial commissioning can last for years after occupancy while it is still not guaranteed to function correctly and optimally as specified. Therefore, tools are necessary to model the correct and optimal functioning of the HVAC system in its environment as closely as possible to detect faults and identify opportunities for improvements. Possible faults can be design and construction faults, degradations during the life-cycle and improper use or maintenance.

Faults manifest themselves in a *fault detection* phase as failures that have to be mapped back to the causing faults in a *diagnosis* phase. Both phases together are called FDD. Continuous commissioning® (CCx), as we understand it, goes beyond FDD by monitoring component performance degradation, evaluating the effectiveness of control sequences, predicting the possible waste of energy and managing assets to improve building performance through maintenance. CCx also includes reprogramming the building automation system to achieve optimal comfort performance and energy efficiency. Opportunities for optimizations are alternative control strategies including set-point optimization and replacement of suboptimal system components, for example variable frequency drive (VFD) pumps instead of constant flow pumps with bypass valves.

The paper gives a brief review on the existing HFM-FDD approach. The main body of the paper describes the energy related extensions of HFM-FDD. Simple models for energy consumption are introduced. A complex real test system is introduced to show results that are based on real data. For the continuous control optimization feature, experiments show how it can be used, but not all possible optimization strategies.

APPLICABLE WORK OF OTHERS

Until now, there has been no simple tool offered by building technology vendors or energy service providers, which can give building facility managers the view

they need to catch building electrical or mechanical system degradations when they occur, not to mention the sub-optimal control sequences as designed. Over the last several years we have observed the emerging of a wave of service practices in the building continuous commissioning area. Standard industrial practices draw both building energy data and weather data into a data warehouse. Energy performance tracking tools are used to normalize the building metered data, analyze energy usage patterns, and issue a system fault report. Most of the time, a degradation of 'whole' system performance can be detected, named as an anomaly. However, the exact cause of the anomaly cannot be easily identified without knowing the exact mechanical and electrical equipment specifications and sub-metering them (Ulickey, 2010).

In academics, researchers have been dedicated to fault detection and diagnosis methods based on both top-down and bottom up approaches. Abrupt hardware faults (stuck damper, leaking valve, and frozen sensor) are relatively easy to detect and identify. However, long-term performance degradation (fan, chiller, compressor COP degradation, air filter clogging) is difficult to catch until a failure occurs. There are studies reported only for individual system performance degradation detection. Rossi and Braun (1997) developed a technique that uses only temperature measurements to detect and diagnose five commonly occurring faults in rooftop air-conditioning systems. Sun et al. (2011) have presented Statistical Process Control (SPC) and Kalman Filtering method to detect chiller gradual capacity degradation based on fixed means and control limits given from system specifications. Meanwhile, although controls error account for 21% occurrence of faults (Breuker 2000), there is no automated way reported so far to detect inefficient control sequences. For example, improper utilization of outdoor air, simultaneous heating and cooling are seldom addressed.

HFM-FDD BASICS

The whole system is based on a graph representation of the system under observation (SUO), in this case an HVAC system installed in a building with its environment. The graph is called a heat flow model (HFM) because it models basically the components of the SUO and the flows that are responsible for heating, cooling, and air quality. The HFM model has been introduced by Zimmermann et al. (2010).

Software system implementation

A basic advantage of this mapping of a real system into an HFM is that it allows for automatic translation of a BIM (building information model) of the SUO into the corresponding HFM to save engineering effort (Lu et al. 2010). The HFM is represented as an xml file that can also be created and edited manually if complete BIM representations are not available.

The generation of the fault detection and diagnosis system from HFM is automated. All HFM nodes and node flow connections are represented by java classes. The node classes are generic using parameters, resulting in a reasonably sized node and connection class library. Specialized nodes can be easily created by using java inheritance. A generator reads the HFM model and instantiates the HFM-FDD runtime system automatically, using this class library.

Node classification and functionality

All flow nodes can be classified in three ways: *simple*, *combined*, and *complex* nodes; *gas*, *fluid*, and *control* nodes; *transformation*, *sensor*, and *distribution* nodes.

A few examples explain the classification: a duct with a temperature sensor is a simple air flow sensor node. A cooling coil is a combined air and water flow transformation node with a controlled actuator. A reheat VAV is a complex node combining a simple air flow transformation node (damper), a simple air flow sensor node (air volume flow rate), and a combined air water node, the reheat coil. Simple air or water distribution nodes are duct or pipe branches and joins without sensors or actuators. An AHU control node is a simple node that computes control signals for the dampers in the economizer and the chilled water valve in the cooling coil.

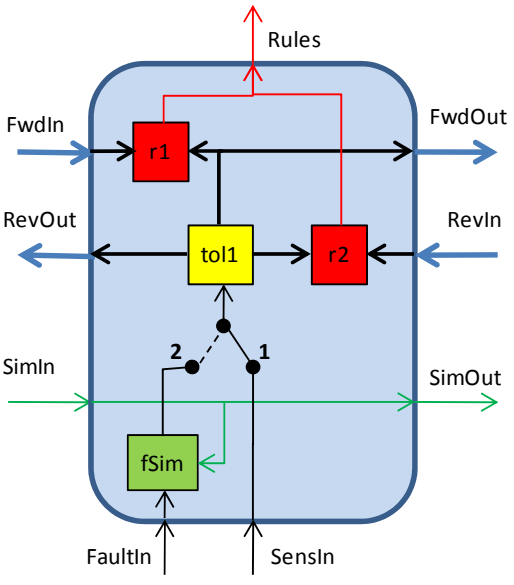

Figure 1 Sensor duct node

A good node to explain the basic principle of FDD is the air temperature sensor duct node. Figure1 shows the structure. The node shows flow in- and outputs left

and right, data inputs at the bottom and rules outputs at the top. The blue flow arcs connect the node with up- and downstream nodes. The arrows marked *Fwd* propagate values downstream, the ones marked *Rev* upstream (against the air flow direction). Each arrow represents a *vector of intervals*. For air, vector components are air dry bulb temperature, humidity ratio, mass flow rate, pressure intervals. Each interval represents the probable valid range of a variable.

For a sensor, the range is defined by the sensor tolerance. For example, if a temperature sensor has a tolerance of 0.5°C and shows a value of 16°C, we assume as interval [15.5, 16.5]. In Figure 1, the sensor value from the SUO comes in real time from the Building Automation System (BAS) or from a trend file trough port *SensIn*. The function *tol1* applies the tolerance, a parameter in the xml HFM. The resulting interval is propagated as *FwdOut* and *RevOut* to the connected flow nodes. The interval is also propagated to the *r1* and *r2* functions.

r1 and *r2* represent failure rule functions. They execute fault detection and evaluation. A fault is detected when the two intervals that enter a failure rule function do not overlap. This very simple and generic principle is illustrated by an example: Let us assume, upstream of this sensor is a cooling coil. Using a coil model and various inputs to the coil, the discharge temperature interval of the coil has been estimated as [11.3, 14.6]. If the sensor shows [15.5, 16.5], the intervals do not overlap and a fault has to assumed. As a measure of the severity or probability of the failure, a failure value is calculated as the distance between the intervals, 0.9 in this example. In the case of overlap, the value is zero.

Failures and faults form an n:m relation. Each fault can cause several failures, represented by a failure vector. The vector resulting from fault detection is called *detection failure vector*. Fault diagnosis is the task to find the fault that most probably caused the failure vector. For this purpose a set of possible failure vectors is provided, one for each fault from a given fault list. If this set is created by fault simulation, the created vectors are called *simulation failure vectors*. Pattern matching is used to find the best match between the detected and a simulated failure vector from the set and thus finding the most probable fault. The quality of the match is expressed as *score*.

Instead of a static set of simulated failure vectors, we create the set dynamically at every data time step to react to dynamic conditions such as outdoor weather, occupancy, and dynamic set-point changes. Therefore, every node executes fault simulation steps based on a component model. In Figure 1 this part is colored green. As possible sensor faults positive or negative offsets are assumed and applied in function *fSim*. This offset does not change the simulated value, for example the air temperature, which is just propagated from *simIn* to *simOut* in the temperature sensor example. By setting the switch in Figure 1 to position 2, the faulty sensor value is propagated to the detection part of the node, in this case to the rule functions. The rule functions create the simulation failure vector components for the node, one for each fault of the fault list. All components are centrally collected and used for the matching process. See also (Zimmermann et al. 2011).

Dynamic system behavior

The system starts by reading the xml HFM file and creating the runtime code. In *the fault detection system mode* a data sample is entered. The data are directed to the related flow nodes according to information in the xml HFM file. The nodes execute estimation, propagation, and rule evaluations. As shown in Figure 1 the node inputs are forward or reverse flow data as well as sample data. Deadlocks and order dependencies are avoided by data synchronization.

When all data of a time step have been processed, the system mode switches to *control simulation*. This new feature has to be explained. Rules regarding flow values, such as temperatures or flow rates, depend on redundant sensors and physical estimation models, e.g. the temperature drop of a cooling coil and sensors at in- and output. For control signals we use a different, simulation based approach. The HFM-FDD provides, as explained, a fault simulation capability. This requires the simulation of the control system. If no fault is inserted, correct control signals are generated.

One simplification made in this approach is the quasi-steady-state-assumption. Changes occur so slowly in HVAC and building systems that no dynamic effects have to be modeled. This has the advantage that the problem of algebraic loops in the simulation can be iteratively solved. Loops exist in air and water flows, but also in the feedback control loops. By allowing the distributed simulation engine to break algebraic loops by inserting iteration delays, stable conditions can always be reached. Especially for the controllers, simple integral behavior with small factors to avoid oscillations will always reach optimal steady states after sufficient iterations. It has been experimentally shown that 30 iterations have always been sufficient.

Using this simple simulation approach, control values for all actuators are generated, using the design control strategy, and applied in failure rules to detect controller errors. During the control simulation system mode, as many real sensor and set-point data as possible are inserted into the simulation providing they do not interfere with the process in the control loop. For example, in the AHU, the real return air temperature and

the supply air temperature set-points are used to keep the simulation close to reality, the mixed air and the cooling coil output temperatures are simulated because they are in the feedback loop.

Similar new *optimization system modes* are introduced to allow ongoing experiments with possible SUO improvements and resulting gains and costs. The same care has to be taken as in the control simulation mode to keep the system as close to reality as possible without interfering with the optimization goal. Examples will be given in section *Optimization results*.

The next system modes are alternately the fault simulation and the evaluation modes. In each fault simulation mode, a single fault is inserted, in the evaluation mode, the simulated values are propagated to the rules to create the simulation failure vector and to calculate the score for this vector. This pair is executed for all faults in the fault list and ordered by rank in a final scoring system mode as explained above. Experiments with different scoring metrics are presented in (Schiendorfer et al. 2012).

All system modes are extended beyond classical FDD by power and energy consumption calculation capabilities to detect energy waste and optimization opportunities as shown in the following sections.

Calibration and tolerances

The HFM is based on simplified physical models. The extent of simplification depends on the provided knowledge about the SUO. In many real cases the documentation is incomplete, detailed physical model parameters are not provided, the system cut sheets to not comply with the constructed reality. Therefore, more precise simulation models are not applicable or would require unreasonable engineering efforts. For each system, model simplifications are chosen according to the situation. The situation is complicated by insufficient instrumentation and especially the lack of predictable knowledge about user behavior. Therefore, FDD with CCx is possible and useful, but the results have to be interpreted with the necessary caution.

If enough reliable trend data exist, models and parameters can be refined using data analysis methods. Examples are provided below.

APPLICATION EXAMPLE

The application used to test the system is a new building extension in Berkeley, CA, with 10,000 m^2 gross floor area (GFA) on 7 levels and 157 zones that are air-conditioned by 2 AHUs. Each zone has an individually controlled reheat VAV. About 70% of the GFA is net internal area (NIA), mainly for offices. The AHUs share a chiller and all reheat VAVs share a hot water supply.

To demonstrate the practicality of the HFM-FDD extensions with real data, 3 of the 157 zones have been modeled together with the 2 AHUs and the 2 water supplies. This is the SUO for the experiments.

Instrumentation

Each AHU is equipped with return, mixed, and supply air temperature sensors, a return air humidity sensor, return and supply air volume flow rate sensors, return and supply fan power meters, and several pressure sensors. Each VAV is supplied with an air flow rate sensor, and each space with an air temperature sensor. The water supplies have supply and return water temperature and pressure difference sensors. Outdoor air temperature is monitored, but not the humidity.

Trend data

Continuous commissioning starts with or shortly after the initial commissioning. Therefore, it cannot be expected to have long-term trend data. In the actual case, we use 2 files with 5 days each of trend data starting 10/13/2011 and 1/11/2012. Both data sources have a sample time of 1 minute and cover 105 data points. Since the data do not include outdoor relative humidity measurements, they have been augmented by data from a Berkeley weather station.

In order to be able to calculate full year results, such as cooling energy, cost of unrepaired faults, or gains from more efficient components or control sequences, an artificial full year data file has been created. The file covers 1 day for each month with 10 samples per hour. To simulate typical site environmental data, outdoor temperature distributions have been calculated for each month of the year using the Berkeley weather data from 2010 and 2011.

Using the month frequency in each bin for 1°F intervals, a corresponding number of trend data samples with outdoor air temperatures in the bin range have been selected in randomized order together with corresponding humidity data. Results of this full year data file will be shown.

POWER RELATED NODES

The HFM of the SUO contains 58 nodes. Of these nodes, only a few types are directly connected with energy consumption: the economizers, cooling coils, and fans of the AHUs, the reheat VAVs and spaces of the zones, and the chilled and hot water supplies.

The **economizer** is performing the simple task of mixing return air with outdoor air. For this purpose it has basically 3 air dampers: *DE* the exhaust, *DB* the by-

pass, and *DO* the outdoor air damper. To guarantee sufficient fresh air, the SUO has a second outdoor air damper *DOmin* in parallel to *DO* that is set to a fixed position. The dampers are controlled with the goal to create a mixed air stream that minimizes the mechanical cooling and heating power requirements. The SUO uses a strategy called *Common High-limit Dry-Bulb Temperature-Based Economizer Logic.*

Simple air mixed temperature models assume that the air flow rates *Qba* through *DB* and *Qoa* through *DO* are

$$Qoa = udv * Qsa \quad (1)$$

$$Qba = (1 - udv) * Qsa \quad (2)$$

With *udv* the damper control value and *Qsa* the supply fan flow rate, resulting in the mixed air temperature *Tma* in relation to the return air temperature *Tra* and the outdoor air temperature *Toa*:

$$Tma = \frac{Toa*Qoa+Tra*Qba}{Qoa+Qra} \quad (3)$$

Equations 1 and 2 assume linear damper to flow ratios and balanced pressure differences over the dampers. In the case of the SUO this is not the case. The supply fan flow rate *Qsf* is much larger than the return fan flow rate *Qrf* so that balanced pressures cannot be assumed.

A new flow model has been derived using electrical equivalences: current for flow rate, voltage for pressure, and electrical resistance for damper air flow resistance. Figure 2 shows the model.

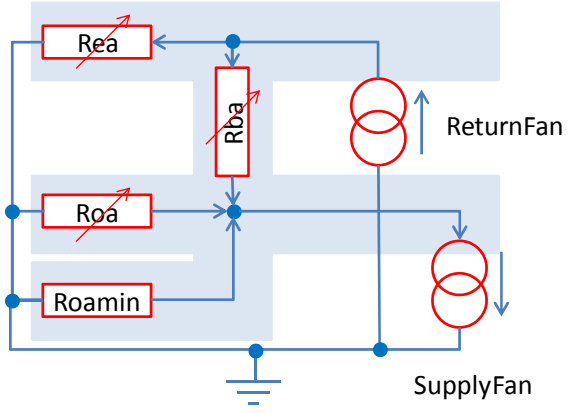

Figure 2 Electrical model of economizer

Using Kirchhoff's laws all currents can be calculated knowing the flows of the return and the supply fan and the relative values of the resistors. The resistors are assumed to be

$$Rea = Roa = 1/udm \quad (4)$$

$$Rba = 1/(1 - udm) \quad (5)$$

The model corresponds well with measured trend values and provides, after another transformation, air mass flow rates *mxa* in all branches. Under the assumption that the air cannot flow backwards through the exhaust damper and based on the return and outdoor air temperatures, the mixed air temperature is:

$$Tma = \frac{mba*Tra+(moa+moaMin)*Toa}{mba+moa+moaMin} \quad (6)$$

The model can also be used to calculate the fraction *foa* of outdoor air in the supply air flow:

$$foa = \frac{moa+moaMin}{moa+moaMin+mba} \quad (7)$$

This fraction is important to calculate the minimum air flow in occupied spaces to guarantee air quality according to (AHSRAE 62.1). The minimum flow is limiting the energy savings of the AHU fans if less flow is required for heating or cooling.

Equation 6 is not exact if the return and outdoor air flows have different humidity ratios *Hrra* and *Hroa*. If these are known, specific enthalpies *hx* are calculated and replace the dry bulb temperatures:

$$hma = \frac{mba*hra+(moa+moaMin)*hoa}{mba+moa+moaMin} \quad (8)$$

From *hma*, *Tma* and *Hrm* are calculated and passed to the connected nodes.

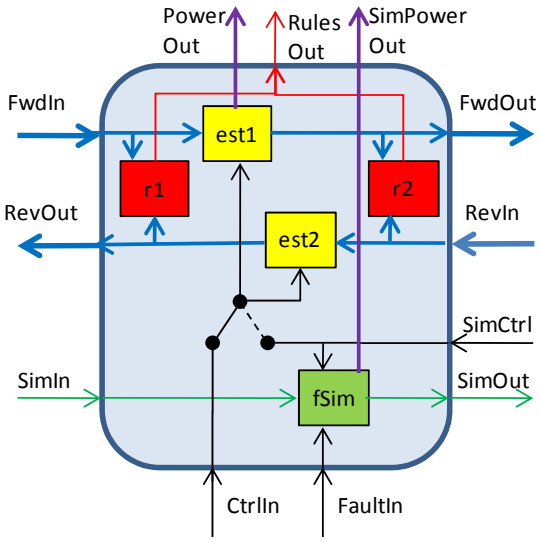

Figure 3 Transformation node with power calculation

The node classification of the economizer is a simple air transformation node as shown in Figure 3. The power out exits do not apply because, although the economizer has large influence on the power consumption, it does not consume power itself.

The estimation function est1 and est2 transform the input flow intervals as a function of the control input *CtrlIn* into output intervals, e.g. *Tma* using Equations 4, 5, and 6 in the forward flow direction or Equation 8 instead of 6. The equations are extended to calculate intervals taking input intervals, damper nonlinearities, parameter tolerances and other uncertainties into account.

In the control simulation mode, the function *fSim* transforms average *SimIn* or measured values into *SimOut* values as a function of *SimCtrl* values to close the controller feedback loop. Not shown in Figure 3 is a rule that compares *CtrlIn* with *SimCtrl* to detect controller faults.

In the fault simulation mode, faults *FaultIn* are introduced into *fSim* and *SimCtrl* replacing *CtrlIn*. Typical economizer faults are stuck or leaking dampers.

The **cooling coil** is a combined air and water transformation node. The basic physical model is Equation 9:

$$Tca = Tma + ccf * ucc * (Tchws - Tma) * pchw \quad (9)$$

Tca is the discharge air temperature, *ccf* a factor that is deducted from trend data, *ucc* the control value, *Tchws* the chilled water supply temperature and *pchw* the water supply differential pressure.

For the cooling power calculation, dehumidification has to be taken into account when *Tca* is below the dew point for *Hrma*. In the case of a wet coil, the humidity ratio *Hrca* is calculated assuming a relative humidity *rHca*=100%. The heat flow removal power *Pcc* of the coil is:

$$Pcc = masf * (hma - hca) \quad (10)$$

masf is the mass flow rate of the supply fan, *hma* and *hca* are the specific enthalpies of the incoming and outgoing air flows. The enthalpies are calculated from the air temperatures and humidity ratios using standard equations. *Pcc* is not the primary power needed for cooling. In the case of a compressor chiller with cooling towers the electric power for the compressor can be a factor of 5 lower (COP=5 at optimal load conditions), but the power for the pumps and blowers has to be added. A detailed chilled water supply model is under development and will be added.

The **supply fan** is a pressure controlled variable frequency drive (VFD) fan wall with 9 fans with a maximum electric power consumption of 64 kW. The electric power consumption *Psf* is measured and recorded as a data point. For simulation purposes an exponential function has been derived from trend data by curve fitting for constant pressure. This is a good example for applying simple calibration methods.

The **reheat VAV** is equipped with a flow sensor, but no discharge air temperature sensor. This lack of a temperature sensor makes it difficult to calculate the reheat power. With the simulation model of the VAV *TdaSim* is calculated for heating power estimates

Space: Very little is known about the zones of the SUO. Floor plans show the 7 floors and the usages of the rooms. Tables show the assignment of rooms to zones with VAVs. In the HFM, spaces and zones are related 1:1. The floor plans allow the calculation of floor area and outdoor wall length. No information about sun shading, wall or window materials are supplied. Also, no occupation schedules are defined. Strongly varying occupancies have to be expected at all times. Together with unknown solar radiation loads, the model assumes a large heat load interval.

RESULTS

In addition to fault detection, the extended HFM-FDD system can be used in two ways to evaluate the power consumption of the SUO:

- Full year energy consumption data for individual components and total cost based on a full year artificial measured data file
- Short term power data using the current or recent samples.

In both cases the results of measured data are compared with simulated data, the latter either without an assumed fault to get optimal design performance or with an assumed fault to analyze fault consequences. In addition, the model parameters, functions, or node types can be modified to test the effect of possible optimizations.

Short term power data are useful for continuous observations for CCx, whereas full year data are mainly useful for optimization proposals. Short term power data together with model changes can also be used for dynamic situation dependent optimizations, e.g. weather dependent set-point changes.

Table 1 Full year heat flow energies in MWh

case	*Ecc A*	*Ecc B*	*Esf A*	*Esf B*	*Erh*	*Etot*
Real	928	280	118	132	69	561
Sim1	103	103	48	48	32	169
Sim2	197	197	106	106	0.27	291
Sim3	292	292	241	241	0.77	600
Sim4	133	133	172	172	0.79	398
Sim5	295	295	78	78	0.96	275

The full year results are collected in Table 1 and will be interpreted in the following paragraphs. All data are extrapolations of using the 12 day artificial data file to 365 days. It has to be observed that column *Etot* is not the sum of the heat flow energies, but the cooling coil data have been divided by an assumed COP=5 of the chiller to represent electrical energy consumption.

The full year heat flow energies *Ecc A* and *B* of the cooling coils with measured data are shown as case *Real*. Although both AHUs are identical, cooling coil A consumes 3 times as much energy as coil B.

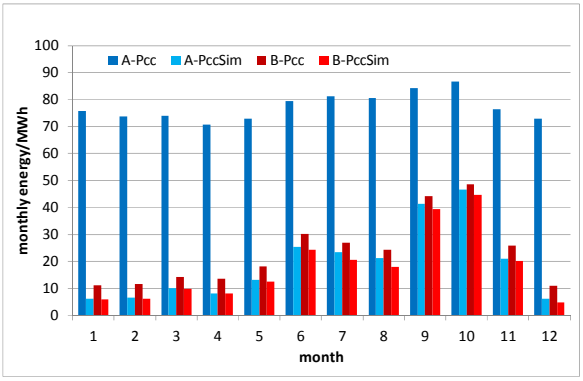

Figure 4 Enthalpy based monthly cooling energies of AHU A and B, measured (Real) vs. simulated (Sim2)

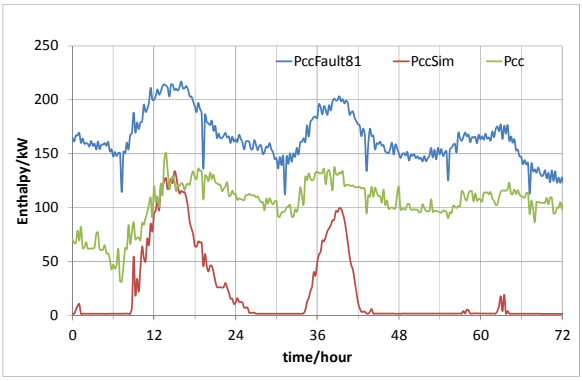

Figure 5 3-day AHU A enthalpies: measured: Pcc, simulated: PccSim, 20% leaking valve: PccFault81

Figure 4 clearly shows that AHU A excessively cools even in winter months. Fault analysis shows that the cooling coil valve is leaking at all times. This is confirmed by the short term fault simulation result in Figure 5 that shows a good correlation between the measured values *Pcc* and the fault simulation *PccFault81*. The correct simulated values *PccSim* show a behavior as expected: Cooling only during daytime. From the *Real* data in Table 1, it can be assumed that AHU B works correctly.

The two supply fans SF A and B are very large power consumers. The necessary air flow rates of all connected VAVs together determine fan powers. The minimal VAV air flow rates are set by fixed lower limits to guarantee air quality requirements. The actual electrical energy consumption is considerably higher than the electrical energy for cooling if compared to AHU B and considering a COP=5 of the chiller.

The total energy for all reheat coils *Erh* cannot be directly measured without discharge air temperature sensors in the VAVs. The shown values are based on estimated *Tda* values. Also, the values are extrapolated from 3 to 157. So these data can only be used for relative comparisons in this prototype experiment.

Because of the uncertainty of the heat load conditions of the spaces, the cases *Sim1* to *Sim3* show simulation results with minimum, average, and maximum space load assumptions. It can be seen that in the case of *Sim2* and *Sim3* no reheating is necessary, *Sim1* shows that reheat power is necessary, but all energy consumers use less energy than in the real case. This result can be interpreted as an indication that in the real system there is much room for repairing not only AHU A but also improving the VAV control strategies and to require the users to turn off as much electrical load as possible during unoccupied times. The three simulations also clearly show that the total energy consumption reacts very sensitively to a change in one component, in this case the heat load of the spaces. Without simulation this behavior would be very difficult to predict.

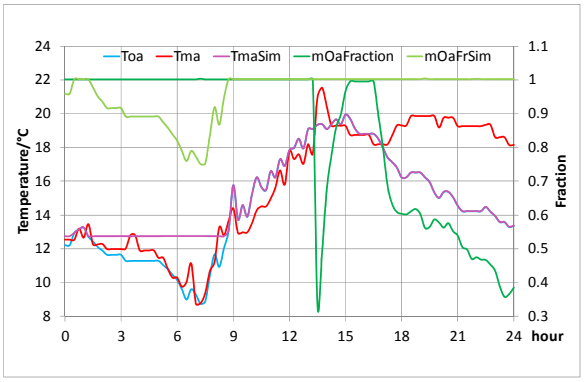

Figure 6 Outdoor air fraction of mixed air of AHU-A

Looking at the outdoor air fraction of the mixed air flow for a day in January 2011, a failure of the economizer of AHU-A becomes obvious. Figure 6 shows that during morning hours the mixed air temperature *Tma* goes much below the supply air set-point of 13.3°C and in the late afternoon stays above the set-point although the outdoor air temperature goes down. This may mean extra VAV reheat power in the morning, but in any case extra cooling power in the afternoon and evening. The simulation *TmaSim* shows the optimal behavior.

This failure has a second implication: the outdoor air fraction is lower than necessary, meaning possibly higher VAV air flow rates and therefore higher supply fan power consumption. The simulation result *mOaFrSim* demonstrates the high optimization possibility for reducing the airflow into the spaces. The real amount can be principally computed by the system, currently this is very imprecise because the VAVs have no discharge temperature sensor. Estimation is done but based on imprecise space load data.

Another economizer optimization strategy is the use of enthalpy based switchover points between fully open and fully closed outdoor air damper. Taylor and Cheng (2010) have shown that this strategy results in unsatisfying operation if sensor tolerances are high. Our data show for example in Figure 6 that this is the case. *Tma* and *Toa* should overlap precisely from 0 to 12 because the outdoor air damper is fully open. Therefore, this optimization option has not been implemented.

A more promising optimization is based on set-points. A HVAC system uses many fixed set-points, e.g. for supply water and air temperatures, space temperatures, water supply differential pressures and fan air pressures. All set-points have influence on the total power consumption, either on pump and fan power consumption, on chiller and boiler COP or on cooling and heating coil heat flows. Table 1 shows a simple experiment with the same load as *Sim2*, but the supply air set point increased by 2°C (*Sim4*) and decreased by 2°C (*Sim5*). Because of resulting changes in supply air flow rates, decreasing the set-point requires less total energy. Cascia (2000) has developed an analytical method to calculate the chilled and hot water supply and the air supply near-optimal set-points based on measured data for installed compressor chillers and the existence of more sensors in the AHUs. Since we do not have this information and these sensors are not installed, we cannot show results of this strategy currently.

CONCLUSION

It has been shown that the extension of the HFM-FDD system yields important power and energy consumption data for continuous commissioning® (CCx). The data can be short term data for comparing the current real consumption with a simulation of adapted models with optimal behavior, data for the near history, or full year estimations using an artificial data file. For the cost analysis of detected faults, results can be obtained inserting these faults into the simulation. In special system modes, experiments with optimization strategies or improved components can be performed using the simulation instead of the real system. We believe that this extension can greatly simply and improve the HVAC system maintenance with the goal to guarantee optimal performance.

REFERENCES

ASHRAE 62.1 Ventilation for Acceptable Indoor Air Quality, ASHRAE Standard 62.1 2010

Breuker, M., Rossi, T., and Braun,J. E., Smart Maintenance For Rooftop Units, ASHRAE Journal Nov. 2000.

Cascia, M.A. 2000. Implementation of a near-optimal global set point control method in a DDC controller, ASHRAE Transactions 2000; Volume 106, Part 1, pp. 249 – 263

Lu, Y., G. Zimmermann, and G. Lo. 2010. Fault Detection and Diagnosis of HVAC Systems Based on a New Heat Flow Model (HFM). Proceedings IAQVEC 2010, The 7th International Conference on Indoor Air Quality, Ventilation, and Energy Conservation in Buildings, Syracuse, USA

Rossi, T.M. and Braun, J.E. A statistical, rule-based fault detection and diagnostic method for vapor compression air conditioners.. International Journal of Heating, Ventilating, and Air Conditioning and Refrigerating Research 3(1):19. 37, 1997

Schiendorfer, A. et al. 2012. Fault diagnosis in HVAC Systems Based on the Heat Flow Model, SimBuild 2012 (to be published)

Sun, B., B. Luh, P., Fellow, O'Neill, Z., and Song, F., Building Energy Doctors: SPC and Kalman Filter-based Fault Detection, 2011 IEEE International Conference on Automation Science and Engineering, Trieste, Italy - August 24-27, 2011

Taylor, S.T. and C.H. Cheng 2010. Economizer High Limit Controls and Why Enthalpy Economizers Don't Work, ASHRAE Journal, November 2010

Ulickey, J., Fackler, T., Koeppel, E., and Soper, J., Building Performance Tracking in Large Commercial Buildings: Tools and Strategies-Characterization of Fault Detection and Diagnostic (FDD) and Advanced Energy Information System (EIS) Tools, California Commissioning Collaborative Report, 2010.

Zimmermann, G., Y. Lu, and George Lo, 2010. Heat Flow Modeling of HVAC Systems for Fault Detection and Diagnosis, Proceedings SimBuild2010, New York City, NY, USA, pp.215-222

Zimmermann, G., Y. Lu, and George Lo, 2011. A Simulation Based Fault Diagnosis Strategy Using Extended Heat Flow Models (HFM), Building Simulation 2011, Sidney, Australia